Composition Fluctuation Effects on Dielectric Normal-Mode Relaxation in Diblock Copolymers. 2. Disordered State in Proximity to the ODT and Ordered State

K. Karatasos, S. H. Anastasiadis,[*,†] G. Floudas, and G. Fytas

Institute of Electronic Structure and Laser, Foundation for Research and Technology—Hellas, P.O. Box 1527, 711 10 Heraklion Crete, Greece

S. Pispas[‡] and N. Hadjichristidis[‡]

Chemistry Department, University of Athens, Zografou University City, 157 01 Zografou, Athens, Greece

T. Pakula

Max-Planck-Institut für Polymerforschung, P.O. Box 3148, D-55021 Mainz, Germany

Received August 25, 1995; Revised Manuscript Received November 6, 1995[®]

ABSTRACT: Dielectric relaxation spectroscopy has been used to investigate the block end-to-end vector relaxation in symmetric poly(styrene-*b*-1,4-isoprene) diblock copolymers both in the ordered state and in the disordered state close to the disorder-to-order transition (ODT). Evidence is presented of two new types of dielectrically active chain relaxations by approaching the ODT from the disordered state and in the ordered state. In the ordered state and besides the usual isoprene subchain overall orientation, a new block relaxation process appears with slow dynamics and amplitude that depends on the sample preparation. The slow process is related to the coherently ordered microstructure and is attributed to the relaxation of the conformal interfaces formed in the ordered state; this assignment is supported by computer simulation results. In the disordered state, a bifurcation of the single dielectric relaxation is observed; the total amplitude increases as the temperature approaches the ODT, whereas the high-frequency process shows an apparent weak temperature dependence. The fast process may be related to polyisoprene subchains that feel higher polyisoprene concentrations near the ODT, whereas the slow relaxation mode can be attributed to the induced orientation correlations near and above the ODT, as supported also by computer simulations.

I. Introduction

The rich variety of phase behavior in diblock copolymers has long attracted the interest of the scientific community.[1] The equilibrium phase morphology of diblock copolymers, which consist of a linear sequence of polymerized monomers of chemical species A covalently bonded to a second contiguous linear sequence of monomers of a different chemical species B, is determined by the overall degree of polymerization, N, the overall volume fraction of the A block, f, and the segment—segment Flory—Huggins interaction parameter, χ, which depends on temperature as $\chi = a + b/T$ with $b > 0$. The entropic and enthalpic contributions to the free energy density scale as N^{-1} and χ, respectively, and therefore, the product χN dictates the equilibrium phase morphology for a certain f. For $\chi N << 10$, the equilibrium morphology is a melt with uniform composition (homogeneous or disordered state). As χN increases to be $O(10)$, a delicate balance between entropic and enthalpic factors leads to an order—disorder transition (ODT) toward a microphase characterized by long-range order in its composition with characteristic size of the order of the size of the molecules. At $\chi N >> O(10)$, highly organized periodic domain microstructures are obtained. The resulting morphology below the ODT

is a polycrystalline structure of uncorrelated grains which consist of coherently ordered periodic domains with characteristic size of the $O(\mu m)$.

In a pioneering work, Leibler[2] constructed a Landau expansion of the free energy to the fourth order in a compositional order parameter field $\delta\phi_A(r) = \phi_A(r) - f$, the fluctuation in the volume fraction of A monomers at position r, in order to obtain the phase diagram of diblock copolymers near the ODT in the χN vs f parameter space. In the framework of the random phase approximation (RPA), he predicted the existence of a critical point for $f_c = 0.5$ at $(\chi N)_c = 10.5$, where a symmetric diblock undergoes a second-order phase transition from the disordered to the lamellar phase. Fredrickson and co-workers[3] incorporated the fluctuation corrections in the effective Hamiltonian for a diblock melt in the Hartree approximation and found that the fluctuation corrections, controlled by a Ginzburg parameter,[3,4] $\bar{N} = Nb^6v^{-2}$ (b is the statistical segment length and v is the average segmental volume), lead to a suppression of the symmetric critical mean field point that is replaced by a weak first-order transition at a lower temperature, with the amplitude of the ordered composition profile predicted to be $O(\bar{N}^{-1/6})$ at the ODT. Monte Carlo computer simulation results[5-10] are in qualitative agreement with the fluctuation correction predictions with respect to both the location of the transition and the deviation from the Gaussian behavior near the ODT. As the ODT is approached from the disordered state, an increase of the copolymer chain radius of gyration is predicted due to an increase in the distance between the centers of gravity of the two blocks, i.e., by a polarization of the copolymer chains,[9]

* Author to whom correspondence should be addressed.
† Also at Physics Department, University of Crete, 711 10 Heraklion Crete, Greece.
‡ Also at Institute of Electronic Structure and Laser, Foundation for Research and Technology—Hellas, P.O. Box 1527, 711 10 Heraklion Crete, Greece.
® Abstract published in *Advance ACS Abstracts*, January 1, 1996.

whereas the ensemble average orientational parameter, expressed as the second harmonical Legendre polynomial, shows an orientation correlation of the chains that occurs at a temperature near the ODT.[7,8]

The dynamics of diblock copolymer melts and the influence of the disorder-to-order transition on the dynamics have only recently attracted the increasing interest of polymer scientists.[11] Theory attempted to derive the intermediate scattering function and its relaxation characteristics for diblock copolymers[12] in the disordered state, as well as to investigate the rheological behavior of disordered diblock copolymer melts.[13] Experimentally, rheological investigations[4] probed the substantial fluctuation enhancement of the shear viscosity in the pretransitional disordered state near the ODT where the departure from thermorheological simplicity at low frequencies was attributed to concentration fluctuation effects; theory[13] only qualitatively captured the pertinent features. Dielectric relaxation spectroscopy (DS) has been used to investigate the segmental[14-17] and chain[18-22] dynamics in diblock copolymers both in the disordered[14-16,18-20] and in the ordered state.[17,21,22] On the other hand, neutron spinecho,[23] dynamic light scattering in the polarized[16,24-29] and depolarized[15,16,30,31] geometry, forced Rayleigh scattering,[29,32] forward recoil spectroscopy,[33] and pulsed-field-gradient nuclear magnetic resonance[25,28,29,34] were utilized to identify the mechanisms of relaxation of composition and orientation fluctuations and of the diffusion in both disordered and ordered diblock copolymers.

DS has been used to investigate the block end-to-end relaxation[18-22,35] utilizing a polyisoprene (PI) block, that is a typical type-A polymer in the classification of Stockmayer;[36] i.e., it possesses a dipole moment component along the chain contour. For ordered diblocks, retardation and broadening of the PI-normal mode were observed and attributed to both a spatial and a thermodynamic confinement of the PI blocks in the PI microdomains.[21] In the disordered state and far from the ODT,[20] the polyisoprene block end-to-end vector relaxation functions in poly(styrene-*b*-1,4-isoprene) diblock copolymer melts show a systematic broadening relative to the polyisoprene homopolymer distributions when the temperature is decreased and/or the molecular weight is increased. The broadening was attributed to both composition fluctuation and proximity to the glass transition effects on the normal-mode relaxation; the effects were theoretically accounted for by a new approach that considered both the short-range fluctuations due to chain connectivity, which exist even in homopolymers and are independent of the block–block interactions, and the long-range composition fluctuations in diblock copolymers due to the proximity to the ODT. Theory was able not only to capture the relative features of the distributions but also to quantitatively compare very well with the experimental dielectric spectra.

In this paper, we apply dielectric relaxation spectroscopy in order to investigate the polyisoprene block relaxation in symmetric poly(styrene-*b*-isoprene) diblock copolymers both in the disordered state close to the ODT and in the ordered state. The behavior for well-disordered diblock copolymers has been addressed in an earlier publication.[20] We present evidence for two new types of dielectrically active chain relaxations. In the ordered state, a new block relaxation appears with amplitude that depends on the sample preparation and dynamics much slower than the polyisoprene subchain orientation also observed. The slow process is at-

Table 1. Molecular Characteristics of the Samples

sample	$w_S{}^a$	f_S	M_n	M_w/M_n	N^b	T_{ODT} (K)
SI-120	0.59	0.58	10 300	1.05	121	~330
SI-140	0.44	0.41	11 800	1.05	140	~350
SI-144^c	0.55	0.52	12 200	1.06	144	359
SI-194^d	0.53	0.51	16 400	1.04	194	410
SI-60^e	0.58	0.55	4 450	1.07	57	~140^f
SI-100^e	0.62	0.59	7 600	1.03	92	~212^f

^{a} Weight fraction of polystyrene (S). ^{b} Based on average segmental volume. ^{c} Reference 38. ^{d} Reference 39. ^{e} Reference 20. ^{f} Estimated from Leibler's theory.[2]

tributed to the relaxation of the conformal interfaces formed in the ordered state within the grains of coherently ordered lamellae. This assignment is supported by very recent Monte Carlo computer simulations using the cooperative motion algorithm,[7,8] which are presented elsewhere.[37] On the other hand, as the temperature decreases toward the ODT in the disordered state, a bifurcation of the single dielectric normal-mode relaxation is observed with the total dielectric strength of the two processes increasing at lower temperatures. The high-frequency component shows an apparent weak temperature dependence, whereas the low-frequency peak of the relaxation spectrum displays temperature dependence similar to the temperature dependence of dielectric normal-mode relaxation far above the ODT. The fast process may be related to polyisoprene chains that feel higher polyisoprene concentrations near the ODT due to the increased amplitude of composition fluctuations, whereas the slow process should be attributed to the orientation correlations induced by the proximity to the ODT as also supported by computer simulations.[37]

This article is arranged as follows: following the Experimental Section (II), the results of the dielectric relaxation investigations are presented in section III. In section IV, the data are discussed in relation to the predictions of the simulations. Finally, the concluding remarks constitute section V.

II. Experimental Section

Materials. The poly(styrene-*b*-1,4-isoprene) diblocks, SI, were synthesized under high vacuum in a glass-sealed apparatus at room temperature using benzene as the solvent and sec-BuLi as the initiator with styrene being polymerized first. After the completion of the reaction for both blocks, the living ends were neutralized with degassed t-BuOH. The number-average molecular weights of both the polystyrene (PS) blocks and the diblocks were determined by vapor pressure osmometry whereas the mole fraction of PS was determined by ^{1}H NMR and the molecular weight distribution by gel permeation chromatography. The diene microstructure of SI was predominantly 1,4 and the molecular characteristics of the copolymers are given in Table 1. Copolymers SI-60 and SI-100 have already been discussed in ref 20, and sample SI-144 was discussed in ref 38; SI-194 will be discussed in ref 39.

DS. Dielectric relaxation spectroscopy was used to investigate the collective chain dynamics of the SI copolymers as a function of temperature. This is dielectrically observable due to the finite dipole moment component parallel to the chain contour of the PI sequence. The complex dielectric permitivity $\epsilon^*(\omega) = \epsilon'(\omega) - i\epsilon''(\omega)$ of a macroscopic system is given by the one-sided Fourier transform of the time derivative of the normalized response function[40] $C(t)$

$$\epsilon^*(\omega) - \epsilon_\infty = -\Delta\epsilon \int_0^\infty \frac{dC(t)}{dt} e^{-i\omega t}\, dt \qquad (1)$$

where $i^2 = -1$, $\Delta\epsilon = \epsilon_0 - \epsilon_\infty$ is the relaxation strength, with ϵ_0 and ϵ_∞ being the low- and high-frequency limiting values of ϵ' for the process under investigation. The quantity $C(t)$ is the normalized dipole autocorrelation function

$$C(t) = \sum_{jk}\langle\mu_j(t)\mu_k(0)\rangle / \sum_{jk}\langle\mu_j(0)\mu_k(0)\rangle \qquad (2)$$

where $\mu_j(t)$ is the dipole moment of jth segment at time t. For nonzero dipole moment components $\mu^{\parallel}$ and $\mu^{\perp}$ parallel and perpendicular to the chain contour, respectively, the response function $C(t)$ can be decomposed into contributions of segmental and overall chain orientations. Neglecting cross correlations between segments of different chains, the autocorrelation function $C(t)$ for the ith chain can be written as[41]

$$C(t) \propto \sum_{jk}\langle\mu_{ij}^{\perp}(t)\,\mu_{ik}^{\perp}(0)\rangle + \sum_{jk}\langle\mu_{ij}^{\parallel}(t)\mu_{ik}^{\parallel}(0)\rangle \qquad (3)$$

The first correlation function, $C^{\perp}(t)$, is sensitive to segmental motion, whereas the second function, $C^{\parallel}(t)$, represents the end-to-end vector correlation function

$$C^{\parallel}(t) = (\mu^{\parallel})^2\langle\mathbf{R}_i(t)\mathbf{R}_i(0)\rangle \qquad (4)$$

where $\mathbf{R}_i(t)$ is the end-to-end vector of the ith subchain. The strength $\Delta\epsilon_n$ associated with the dielectric normal-mode relaxation, eq 4, is given by

$$\Delta\epsilon_n = \frac{N_A\,(\mu^{\parallel})^2\langle R_I^2\rangle\varrho w_I}{3M_{n,I}\,k_BT}F \qquad (5)$$

where N_A is Avogadro's number, ρ the mass density, w_I the weight fraction of the active block in the copolymer with $M_{n,I}$ the block number-average molecular weight and $\langle R_I^2\rangle$ the block end-to-end distance, k_B the Boltzmann constant, T the temperature, and F the internal field factor, which for normal-mode relaxation is taken to be unity.[42]

Two different measurement systems were utilized for the dielectric measurements in order to cover a $10^{-2}-10^6$ Hz frequency range: (i) a Hewlett-Packard HP 4284A impedance analyzer based on the principle of the ac-bridge technique to cover the frequency range 20–10^6 Hz;[20,35] (ii) a Solatron-Schlumberger frequency response analyzer FRA 1260 supplemented by using a high-impedance preamplifier of variable gain for the low frequencies, $10^{-2}-10^5$ Hz.[43] The sample resided between two gold-plated stainless steel electrodes (diameter 25 mm) with a spacing of 50 ± 1 μm maintained by two fused-silica fibers 50 μm in diameter; attention was paid to achieving a good contact between the sample and the electrodes. The sample was kept in a cryostat with its temperature controlled via a high-pressure nitrogen gas jet heating system allowing a stability of the sample temperature in margins of ±0.1 °C in a broad temperature range of -160 to $+300$ °C. The absolute values of the loss part of the dielectric permitivity, ϵ'', depend on the accuracy of the value of the sample thickness given to the instrument software. Since the measurements with the two different instruments were performed on two different samples, a way to account for the absolute values of ϵ'' is to normalize the two spectra using absolute values for the real part of the dielectric permitivity, ϵ'.

For quantitative analysis, the generalized relaxation function according to Havriliak and Negami[44] is traditionally used, which provides, in most cases, a satisfactory description of the experimental spectra; the absence, however, of a clear physical interpretation of the adjustable parameters involved and the fitting uncertainties restrict its use solely as a phenomenological way to account for the features of the underlying processes. Besides, an additional conductivity contribution at low frequencies and high temperatures due to free charges has to be accounted for by a power law dependence $\epsilon''(\omega) = \sigma_o/(\epsilon_v\omega^s)$, where σ_o is a fit parameter, $s = 1$ for pure conductivity contribution, and ϵ_v denotes the permitivity in free space. For multiple relaxation processes, use of more than one empirical Havriliak–Negami function is required; this, however, leads to a large number of adjustable parameters in the fitting procedure (four parameters are needed for each Havriliak–Negami function).

A direct transformation of the dielectric data in order to obtain the distribution of relaxation times with no a priori
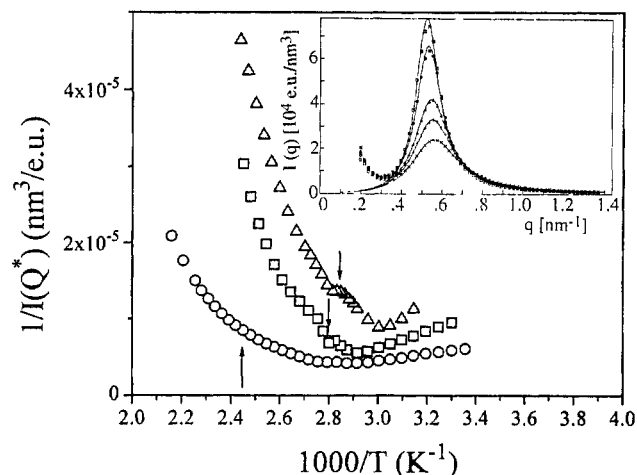

Figure 1. Inverse peak intensity plotted vs inverse temperature for three symmetric diblock copolymers: ($\triangle$) SI-140, ($\square$) SI-144, and (O) SI-194. The arrows indicate the transition temperatures obtained by SAXS and rheology, as discussed in the text. The inset shows the fit of Leibler's mean-field theory to the scattering profiles of SI-140 at various temperatures: (x) 410, (+) 390, ($\triangle$) 380, (O) 361, and ($\square$) 355 K.

assumption of the form of the relaxation function is certainly more appropriate.[45] Recently, we presented a method[20] based on a modification of the widely used CONTIN routine[46] of analysis of photon correlation spectroscopy data[47] for the inversion of the experimental correlation function, with the significant advantage of the routine providing reliable statistical criteria for the support or rejection of the nominal proposed solutions. The method performs an inversion of the experimental $\epsilon''(\omega)$ spectrum in order to determine the distribution of relaxation times $F(\ln \tau)$ by assuming a superposition of Debye processes, i.e.,

$$\frac{\epsilon''(\omega)}{\Delta\epsilon} = \int_{-\infty}^{\infty}F(\ln \tau)\frac{\omega\tau}{1 + (\omega\tau)^2}\,d(\ln \tau) \qquad (6)$$

where $F(\ln \tau)$ is normalized. Alternatively, eq 6 may be written as

$$\epsilon''(\omega) = \int_{-\infty}^{\infty}\tilde{F}(\ln \tau)\frac{\omega\tau}{1 + (\omega\tau)^2}\,d(\ln \tau) \qquad (7)$$

where $\tilde{F}(\ln \tau) = \Delta\epsilon F(\ln \tau)$; integration of the resulting $\tilde{F}(\ln \tau)$ spectrum yields $\Delta\epsilon$, since the $F(\ln \tau)$ distribution is normalized. A similar procedure was subsequently presented by others[48] as well.

Small-Angle X-ray Scattering (SAXS). SAXS measurements were performed for three of the samples of Table 1, SI-140, SI-144, and SI-194, with a Kratky compact camera (Anton Paar KG) equipped with an one-dimensional position-sensitive detector (M. Braum) as described in detail elsewhere.[49] The smeared intensities were collected in a multichannel analyzer and transferred to a Vax computer for further analysis. The data have been corrected for absorption, background scattering, and slit length smearing. The background correction was made by subtracting from the total intensity the contribution of density fluctuations evaluated from the measured isothermal compressibility.[49,50] Primary beam intensities were determined in absolute units by using the moving slit method. The inverse peak intensities for the three samples are shown in Figure 1. In the inset, the scattering profiles of the SI-140 are fitted to Leibler's mean-field theory,[2] which adequately describes the scattering profiles only at high temperatures (410–380 K) but fails as the ODT is approached. At the same time, the inverse peak intensity vs inverse temperature plot deviates strongly from linearity as a result of the fluctuation corrections[3,4] which are important for the small molecular weights used in the present study. The arrows in Figure 1 indicate the order–disorder transition temperature obtained by SAXS (SI-140 and SI-144) and by rheology (SI-144[38] and

SI-194[39]). The identification of the ODT temperature for SI-140 and SI-120 by rheology is impossible because of the closeness of the transition to the glass transition temperature of the polystyrene domains, as will also be discussed later. Indeed, the isochronal temperature measurements of the storage, G', and loss, G'', moduli of the materials at a low frequency (1 rad/s) and constant stress, with strain amplitude kept in the linear viscoelastic regime, for both SI-140 and SI-120 have shown a continuous-like decrease of the moduli with temperature and not the discontinuous change of G' at a characteristic temperature identified with the ODT.[4,38,39] From the peak position and the width of the SAXS data, one can estimate the lamellar period and provide a measure of the coherence of the grains in the ordered state; the lamellar period is 12.1, 12.3, and 14.4 nm for SI-140, SI-144, and SI-194, respectively, whereas the coherence length is estimated in the range 50–80 nm.

III. Results

Ordered State. Figure 2a shows a semilog plot of the loss part of the dielectric permitivity, $\epsilon''(\omega)$, vs frequency for the melt-prepared symmetric ordered diblock copolymer SI-144 in the low-frequency range 10^{-2}–6×10^4 Hz for temperatures 313–338 K, whereas the inset depicts the behavior of the same sample in the higher 20–10^6 Hz frequency range and for temperatures 304–344 K. The higher frequency measurements were needed in order to quantitatively investigate the faster processes with better resolution even at the high temperatures. In the temperature range under discussion, SI-144 resides in the ordered state according to both SAXS and rheological data[38] (ODT at 359 K, Table 1). Besides the high-frequency/low-temperature segmental relaxation in the PI-rich microenvironments that is evident at very low temperatures (not shown), and the lower frequency/higher temperature relaxation, attributed to the usual polyisoprene block end-to-end orientation, a third process is observed at low frequencies and high temperatures with a stronger temperature dependence. The behavior of the two slower processes with temperature is also evident in Figure 2b, where the distributions of relaxation times $\bar{F}(\ln \tau)$, eq 7, for SI-144 in the low-frequency regime are shown in the temperature range where the polyisoprene segmental relaxation is much faster and does not interfere with the data. The quality of the data analysis using the modified CONTIN procedure is shown as a line in Figure 2a through the data at 338 K. The new slow process in Figure 2b shows a stronger temperature dependence than the faster process attributed to the polyisoprene normal-mode motion. In the following, the relaxation times for the new slow process will be obtained from the $\bar{F}(\ln \tau)$ of Figure 2b, whereas they will be obtained for the normal-mode process from the inversion of the dielectric data shown in the inset of Figure 2a. A behavior similar to that for SI-144 is shown for various temperatures in Figure 3 for the ordered SI-194 diblock (ODT at 410 K, Table 1); the slow process is observed less clearly than for the SI-144 due to the interference of the higher dc conductivity contribution at low frequencies. The higher frequency data in the inset of Figure 3a are even more useful in this case in order to acquire measurements with higher resolution, because the normal mode appears only at the edge of the frequency window of the low-frequency system. A composite single spectrum using the data in the two frequency ranges is not attempted in either Figures 2a or 3 because the slower process in both systems depends on sample preparation, as will be discussed in connection to Figure 4 below.

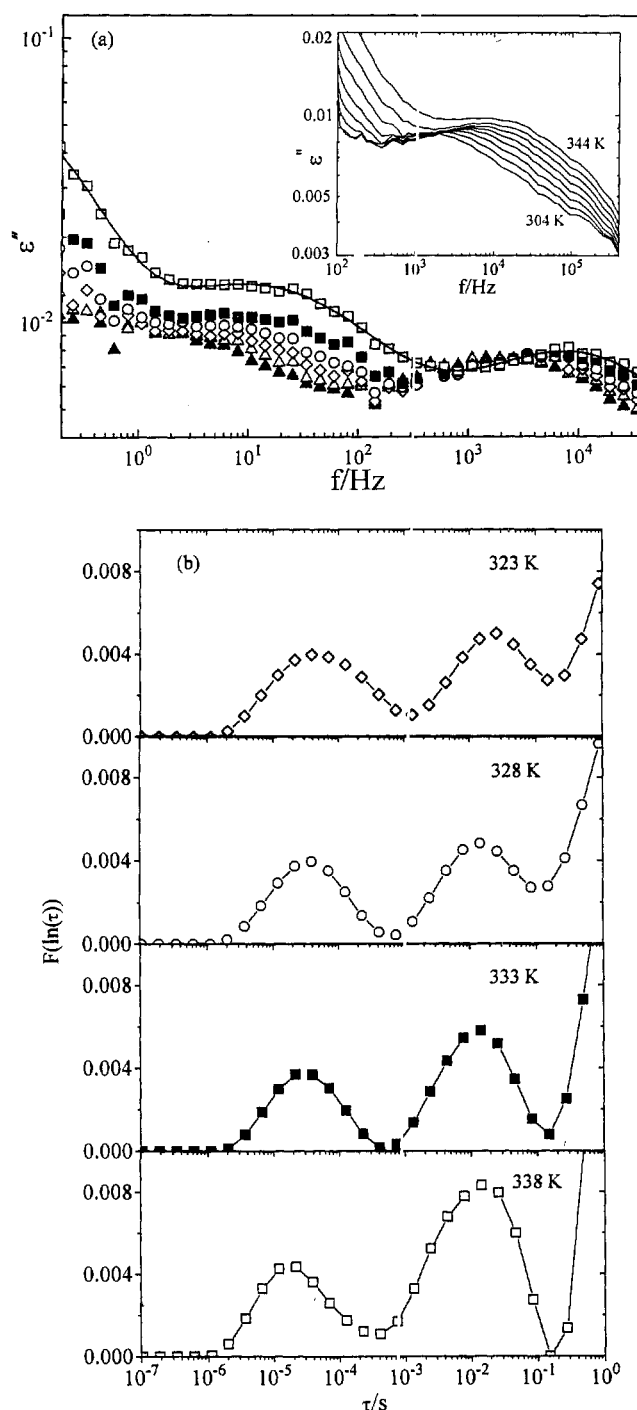A splitting of the normal-mode relaxation has been observed recently in a 30 wt % SI(42–42)/toluene

Figure 2. (a) Frequency dependence of the dielectric loss ϵ'' for the SI-144 diblock copolymer in the low-frequency (10^{-2}–6×10^4 Hz) range for various temperatures: (□) 338, (■) 333, (○) 328, (◇) 323, (△) 318, and (▲) 313 K. The solid line through the data points at 338 K is the fit corresponding to the distribution of relaxation times in (b). In the inset, the data up to the higher frequency range (20–10^6 Hz) for temperatures 304–344 K every 5 K are shown. (b) Distribution of relaxation times $\bar{F}(\ln \tau)$ for SI-144 at various temperatures obtained from the inversion of the low-frequency dielectric loss data at varying temperatures.

diblock copolymer solution (M_v = 84 000, 50 wt % polystyrene),[22] where a slower process suddenly appeared by increasing concentration and/or decreasing temperature and its appearance was related to the ODT. Similar behavior was also observed for a 20 wt % SI-(76–67)/toluene solution (M_w = 143 000, 53 wt % polystyrene).[51] These authors claimed that their fast process was a new relaxation that was related to the
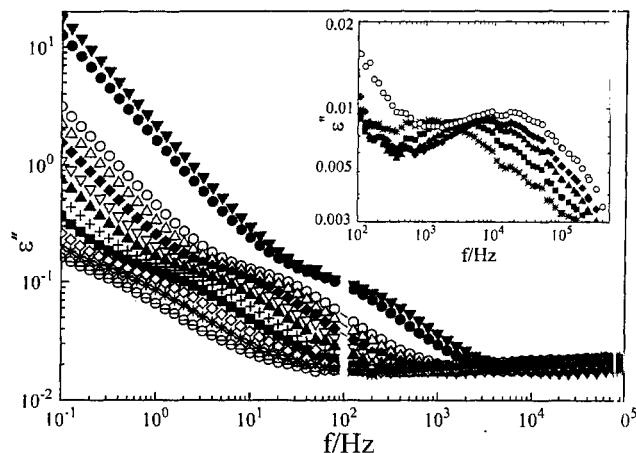
Figure 3. Frequency dependence of the dielectric loss ϵ'' for the SI-194 diblock copolymer in the low-frequency $(10^{-2}-\epsilon \times 10^4$ Hz) range for various temperatures: ($\ominus$) 311, ($*$) 316, ($\diamond$) 321, ($\blacksquare$) 326, ($+$) 331, ($\blacktriangle$) 336, ($\triangledown$) 341, ($\blacklozenge$) 346, ($\triangle$) 351, (O) 356, ($\bullet$) 376, and ($\blacktriangledown$) 381 K. In the inset, the data up to the higher frequency range $(20-10^6$ Hz) for varying temperatures: ($*$) 316, ($\blacksquare$) 326, ($\blacktriangle$) 336, ($\blacklozenge$) 346, and (O) 356 are shown.

ODT and was attributed[22] to SI junction point fluctuations in the interphase region perpendicular to the interface plane, whereas their slow one was the usual end-to-end vector fluctuation due to the motion of the free isoprene ends and was a continuation of the respective process in the disordered state. Both the SI-144 and SI-194 diblocks discussed in the present manuscript reside in the ordered state but close to their respective ODTs (Table 1) in the temperature range of the dielectric measurements. In the following, we will propose that it is the slow relaxation process that is related to the ordered state and we will suggest a mechanism related to the relaxation of the coherent block copolymer interfaces formed below the ODT.

Figure 4a depicts the dielectric loss $\epsilon''(\omega)$ vs frequency for SI-194 for two different sample histories, where the data at certain temperatures are compared for a sample prepared in the melt and a specimen prepared by slow solvent casting. The increase in $\epsilon''(\omega)$ at low frequencies is not related to the usual dc conductivity but is due to the extra slow process that was clearly observed in the low-frequency dielectric measurements shown in Figure 3a. Important differences are observed which are quantified in Figure 4b, where the distribution of relaxation times $\bar{F}(\ln \tau)$ obtained from the inversion of the experimental dielectric loss data is shown. The most probable relaxation times for the new slow process are apparently independent of the sample history, whereas there is a strong dependence of its dielectric strength $\Delta\epsilon$ on the method of specimen preparation; $\Delta\epsilon$ for the specimen prepared from the melt is much lower than the $\Delta\epsilon$ for the specimen obtained by slow solvent evaporation. The differences in these samples should be related to the coherence of the ordered structure; a small grain size of coherently ordered lamellae is expected for the melt-prepared sample, whereas a slow evaporation of solvent allows the development of longer range macroscopic coherence in ordered diblocks.[52] On the other hand, both the relaxation rate and the dielectric strength of the faster process are independent of the specimen preparation method; this mode is attributed to the polyisoprene end-to-end vector orientation fluctuations due to the motions of the free isoprene ends, as will be also discussed later.

Figure 5 shows an Arrhenius plot of the most probable relaxation times obtained from the peak values of the
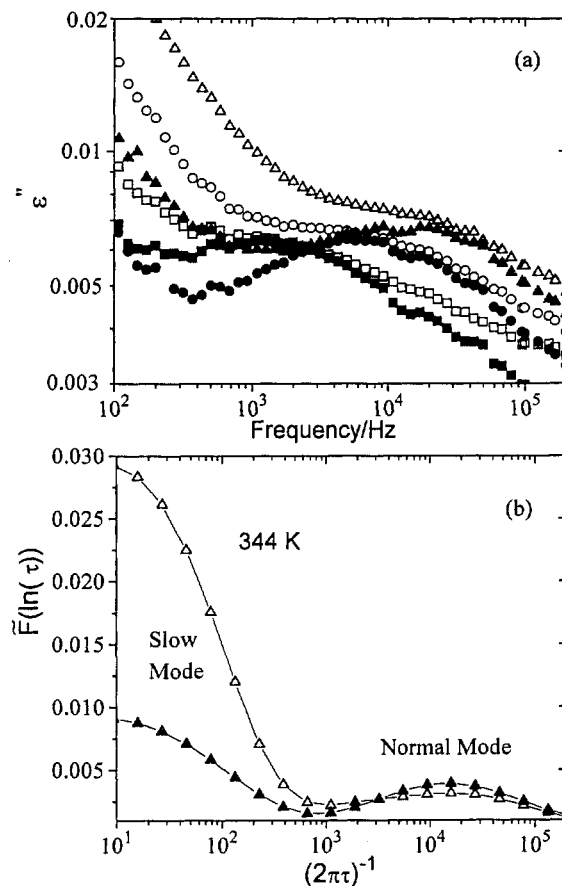

Figure 4. (a) Dielectric loss $\epsilon''(\omega)$ for the SI-194 diblock prepared from the melt (filled symbols) and by slow solvent casting (open symbols) for temperatures 304 ($\blacksquare$, $\square$), 324 ($\bullet$, O), and 344 ($\blacktriangle$, $\triangle$) K. (b) Distribution of relaxation times $\bar{F}(\ln \tau)$ for SI-194 obtained from the inversion of the dielectric loss data for specimens prepared from the melt ($\blacktriangle$) and by slow solvent casting ($\triangle$).

distributions $\bar{F}(\ln \tau)$ for samples SI-194, SI-144, and SI-140 as a function of temperature. The characteristics of the two modes will lead to the identification of the underlying mechanisms of relaxation. As discussed before, the relaxation times of the slow process are almost independent of the sample preparation history and they show a stronger temperature dependence than the faster process; the latter shows a temperature dependence similar to the one for a polyisoprene block in well-ordered diblock copolymers in the bulk[21] and of homopolymer polyisoprene.[41] Therefore, the faster process can be readily attributed to the common polyisoprene block end-to-end vector orientation due to motions of the polyisoprene free ends in the polyisoprene microdomains. This has been shown[21] to be slower than the normal mode of a polyisoprene homopolymer due to the tethering of the isoprene chain to the polystyrene domains (it introduces a factor of 4) and to both spatial and thermodynamic confinement of the chains in their microdomain. The very small differences in the relaxation times of the fast process for the three samples are in agreement with the small differences in the molecular weights of the polyisoprene blocks of the ordered block copolymers.

In Figure 5, we have also included the relaxation rates for the normal mode and for a slow process that was observed at low enough temperatures for two diblocks of ref 21, i.e., SI(12.5−9.5) ($M_w = 22\,000$, $M_w/M_n = 1.06$, 56.8 wt % polystyrene) and SI(14−14) ($M_w = 28\,000$, $M_w/M_n = 1.06$, 50.0 wt % polystyrene). In those systems
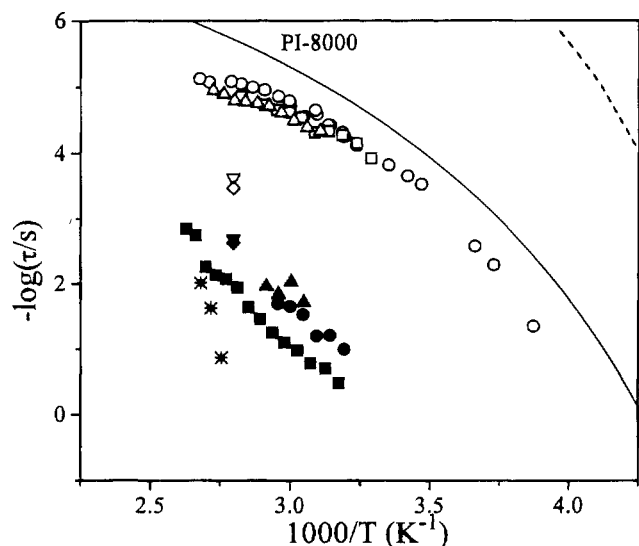
Figure 5. Temperature dependence of the relaxation times of the fast (□, ○, △, ▽, ◇) and the slow (■, ●, ▲, ▼, ◆) process obtained from the peaks of the distribution functions F̄(ln τ) for the following: melt-prepared SI-194 (□, ■), SI-144 (○, ●), and SI-140 (△, ▲) specimens; SI(12.5−9.5) of ref 21 (▽, ▼); and SI(14−14) of ref 21 (◇, ◆). The solid line denotes the normal motion of an polyisoprene homopolymer of molecular weight 8000 (similar to the polyisoprene block of SI-194), whereas (*) denotes the segmental times of the polystyrene-rich environment for SI-144, obtained by depolarized dynamic light scattering. The dashed line shows the measured segmental times of the polyisoprene microdomains.

and besides the normal-mode relaxation, a slower process was evident in the frequency window of the technique (20 Hz−50 kHz) below 357 K for SI(12.-9.5) (Figure 2 of ref 21) or in the temperature plot at 100 Hz (Figure 1 of ref 21) at ~375 K for SI(12.-9.5) and at ~390 K for SI(14−14). The fast relaxation was identified with the polyisoprene subchain relaxation; it is much slower than the normal-mode relaxation in our systems due to higher molecular weights of their polyisoprene blocks. The slow relaxation process was attributed to the segmental motion of the polystyrene blocks in the ordered state since the loss maxima in the temperature plots were located somewhat higher than the estimated glass transition temperatures of the polystyrene blocks. However, the characteristic relaxation times of the slow process (at least based on the two data points that can be extracted from ref 21) shown in Figure 5 do not signify segmental motion of polystyrene. The segmental relaxation of polystyrene can be measured independently by the photon correlation spectroscopy technique of dynamic light scattering in the depolarized geometry due to the high molecular optical anisotropy of polystyrene segments. The relaxation times for the polystyrene segmental motion for SI-144 obtained from the inverse Laplace transform of the experimental correlation function are also shown in Figure 5, and they clearly exhibit a much stronger temperature dependence as expected for segmental motion in the proximity to the glass transition of the polystyrene domains. Note that, for the polystyrene block molecular weights of the copolymers used in the previous investigation,[21] the segmental motions would be even slower because of the molecular weight dependence of the glass transition. Besides, the comparison with molecular simulations,[37] to be discussed below, shows the presence of a slow process in the ordered state even in systems without glass transition effects, and therefore, its origin should be different. Note that the slow process shows a weak sensitivity on the molecular
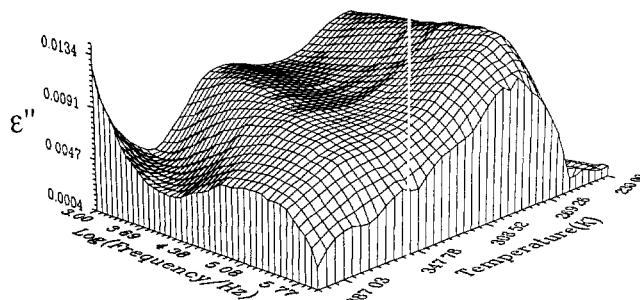

Figure 6. Three-dimensional representation of the temperature and frequency dependence of the dielectric loss ε″ for the SI-120 diblock copolymer in the homogeneous state.

weights of the diblocks, to be discussed in relation to computer simulations later.

Disordered State near the ODT. Figure 6 shows a three-dimensional representation of the loss part of the dielectric permitivity, ε″(ω), for the symmetric diblock copolymer SI-120 in the frequency range 10^3−10^6 Hz and for temperatures 217−400 K. The spectrum exhibits features that are different from typical spectra of homogeneous diblock copolymers[18,20] far from the ODT which show two distinct relaxation processes well separated in the frequency−temperature space, and the conductivity contribution at low frequencies/high temperatures. The high-frequency/low-temperature relaxation displays a strong temperature dependence and is attributed to the segmental relaxation in PI-rich microenvironments of the disordered diblocks,[18] whereas the low-frequency/high-temperature relaxation has been attributed to the PI block end-to-end orientation, i.e., to the PI block normal-mode relaxation in the disordered state.[18−20,35] The distribution of relaxation times for the normal-mode process has been found to be narrower than the respective for the segmental process but still broader than the one for polyisoprene homopolymers of comparable chain length.[20] However, the broad but single relaxation observed at high temperatures in the spectrum of Figure 6, which is attributed to the normal-mode process, shows a long tail toward higher frequencies when the temperature decreases.

This behavior is more evident in Figure 7, where semilog plots of the dielectric loss ε″(ω) for SI-120 are shown vs frequency at two different temperatures. At high temperatures (394 K), Figure 7a, a single but broad relaxation is observed together with the conductivity contribution at low frequencies. The data can be represented by a single Havriliak−Negami (HN) relaxation function[44] plus the conductivity contribution. The HN parameters extracted indicate a significant broadening of the dielectric normal-mode peak when compared to the homopolymer polyisoprene[41] but also compared to homogeneous diblocks far away from the ODT;[20] this is a result of the presence of significant composition fluctuations in the proximity of the ODT. The new feature for SI-120 is the double-peak structure of ε″(ω) at lower temperatures (e.g., 342 K), Figure 7b. The faster peak should not be confused with the much faster PI segmental mode[18] which appears in the experimental frequency window at considerably lower temperatures (see Figure 6). Apparently the description of ε″(ω) requires an additional HN function. Behavior similar to the one reported here, i.e., the appearance of high-frequency shoulder/peak that continuously gains in amplitude besides the normal-mode process, has recently been observed in a 21.3 wt % SI(27−78)/toluene solution (M_w = 105 000, 30.5 wt % polystyrene)[51] and to a lesser extent in a 20.1 wt % SI(32−78)/toluene
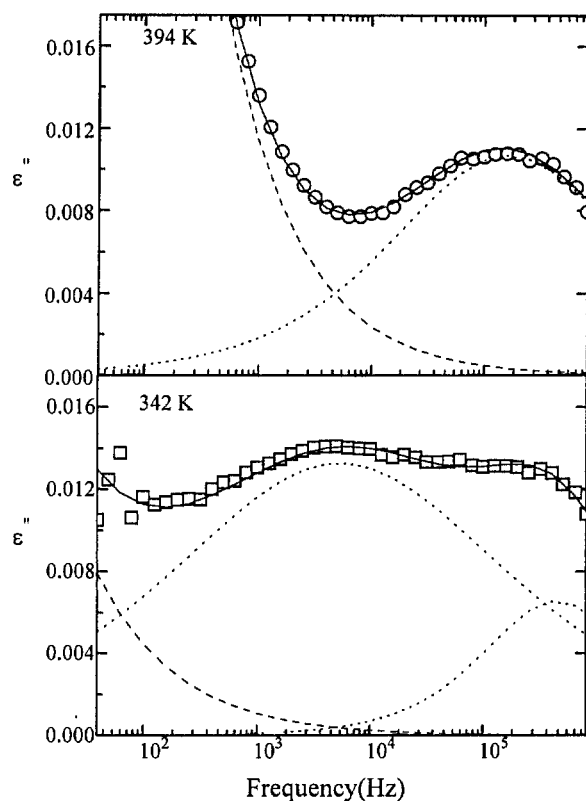
Figure 7. Dielectric loss $\epsilon''(\omega)$ for the SI-120 disordered diblock at 394.5 (a) and 342.5 K (b). The single normal-mode process at high temperatures becomes double at lower temperatures. The dielectric loss data are analyzed with one or two Havriliak–Negami functions plus the dc conductivity contribution.
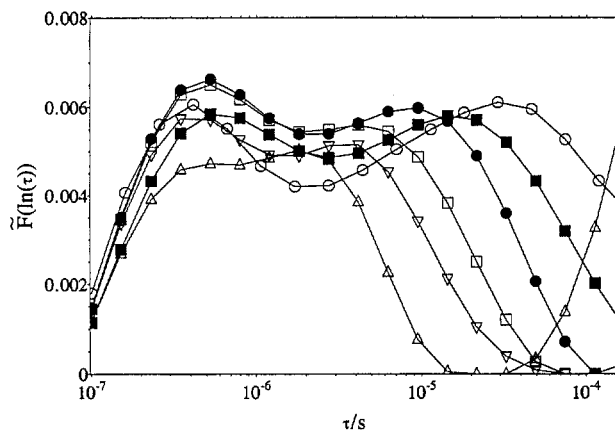

Figure 8. Distribution of relaxation times $\tilde{F}(\ln \tau)$ for homogeneous diblock copolymer SI-120 at various temperatures obtained from the inversion of the dielectric loss data at 400 ($\triangle$), 379 ($\square$), 384 ($\triangledown$), 369 ($\bullet$), 359 ($\blacksquare$), and 347 K (O).

solution (M_w = 110 000, 29 wt % polystyrene).[51] The difference between these two samples is that the former is closer to its ODT than the latter.[26b,31]

Figure 8 shows the distribution of relaxation times $\tilde{F}(\ln \tau)$, eq 7, for the diblock copolymer SI-120 for various temperatures and in the frequency range where the high-frequency and low-temperature polyisoprene segmental relaxation is not interfering with the data for the chain motions. The obtained $\tilde{F}(\ln \tau)$ are very broad even at the highest temperatures investigated with the double nature of the distribution functions being evident even at 400 K; this is much more pronounced at lower temperatures (for example at 359 K). In the following, the relaxation times for the two highest temperatures
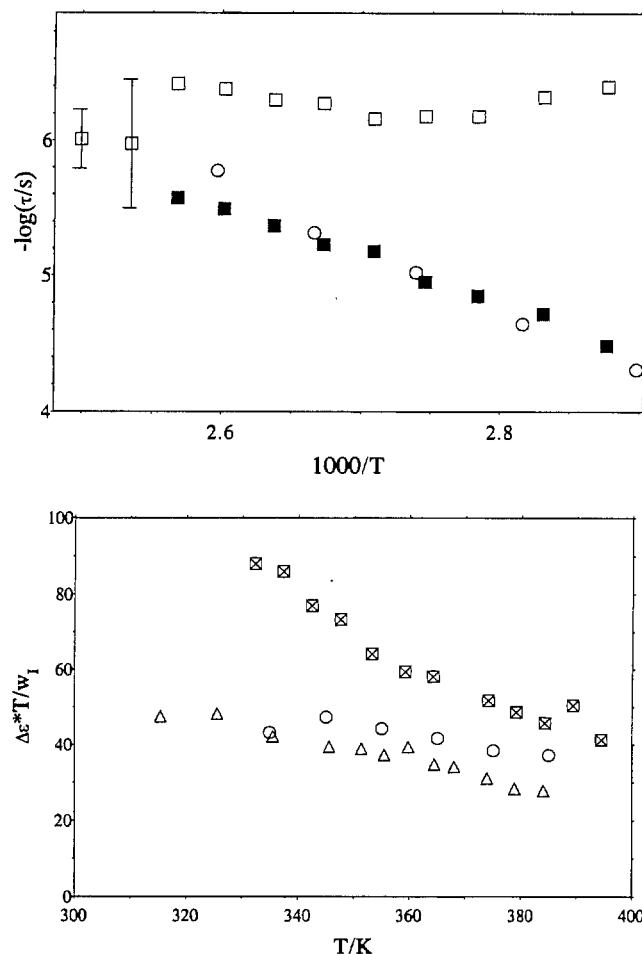

Figure 9. (a) Temperature dependence of the fast ($\square$) and slow ($\blacksquare$) relaxation times obtained from the peaks of the distribution functions of Figure 8 for SI-120. The error bars at the highest temperatures signify the very broad distribution functions. (O) denote the single normal-mode process for a disordered SI-100 far from its ODT.[20] (b) Dielectric strength of the normal-mode process for SI-120 obtained from the integral of the distributions of Figure 8 ($\boxtimes$) and of the well-disordered SI-100 (O) and SI-60 ($\triangle$).[20] The $\Delta\epsilon$ T/w_I abscissa accounts for the normalization of eq 5.

(400 and 395 K) will be obtained by considering the distributions as single but very broad. Figure 8 demonstrates two additional pertinent characteristics of the distribution of relaxation times. The two peaks of the distribution functions exhibit apparently different temperature dependencies; the peak at longer times (low-frequency peak) becomes slower as the temperature decreases similarly to the behavior of the normal-mode relaxation for both homopolymers and disordered diblocks far from the ODT, whereas the new peak at short times (high-frequency peak) is apparently insensitive to temperature variations. Note that the temperature range shown in the figure is sufficiently far from the temperature where the polyisoprene segmental relaxation enters the frequency window of the technique; thus, the isoprene segmental does not interfere with the faster mode shown in Figure 8, as well as in the following Figure 9.

Figure 9a depicts an Arrhenius plot of the relaxation times obtained from the peak values of the distributions in Figure 8 together with the normal-mode relaxation times for the SI-100 diblock copolymer.[20] As discussed above, the fast process of SI-120 shows a very weak temperature dependence whereas the slow process exhibits a temperature dependence very similar to that of the normal-mode relaxation of SI-100.[20] An apparent

insensitivity to temperature variations implies the existence of two competing factors that cancel the effect of temperature on the relaxation time; this strong finding will be utilized below in order to suggest a possible mechanism of relaxation for this process. Figure 9b compares the total dielectric strength, $\Delta\epsilon$, for the two processes of Figure 8, i.e., the integral under the double-peak structure of Figure 8 for SI-120 with the respective values[20] for SI-60 and SI-100. The y-axis representation is more appropriate in that use of $\Delta\epsilon T/w_I$ as the abscissa normalizes the dielectric strength of the normal-mode process according to eq 5. The very weak dependence of $\Delta\epsilon T/w_I$ with temperature for SI-60 and SI-100 (as well as for other diblock copolymers far from their ODT) is expected in view of eq 5. However, the behavior is dramatically different for SI-120, where a strong increase in $\Delta\epsilon T/w_I$ is observed by lowering the temperature. This increase should be related to the effects of the proximity to the ODT on chain extension[3b,4-8] and/or orientation.[30,37] We will show below that the slow process is related to the chain orientation correlations in the proximity to the ODT.

The exact location of the ODT is very important for the discussion of the above findings. Rheology has been shown to be a very sensitive tool for the determination of the order–disorder transition temperature in diblock copolymer melts.[4,38,39] The discontinuity in the isochronal plots of the dynamic elastic modulus G', and to a lesser degree of the loss modulus G'', at low frequencies, corresponding to the terminal region, vs temperature provides a distinct feature for identifying the ODT and is accompanied by a failure of the superposition principle below certain critical frequencies. The presence of the steplike decrease in the G' vs temperature plots signifies the transition from a solidlike (ordered) to a liquidlike (disordered) state. This is usually accompanied by a steplike change in the X-ray or neutron scattering maximum intensity at wavevector q^* by crossing the ODT.[4,38,39] The proximity of the effective copolymer glass transition, T_g, to the microphase separation temperature was shown,[19,53] however, to inhibit the formation of the long-range structure in the ordered state. This is expressed by the absence of the steplike change in the scattering intensity at the maximum of the structure factor now exhibiting a smooth broad change in its slope vs temperature, similarly to the behavior shown in Figure 1 for SI-140; to be more precise, it is the T_g of the polystyrene-rich microphase that inhibits the microphase separation. A similar intervention of the glass transition with the development of large-amplitude composition fluctuations near the temperature of the macrophase separation in polymer blends, even resulting in an inhibition of the phase separation, has been very recently documented.[54] The rheological data for SI-120 show only a broad change in the G' vs temperature plot from a higher to a lower slope at ~60 °C followed by another change back to a higher slope at ~77 °C. This change in the behavior over a broad temperature range can be attributed to the intervention of the T_g with the ODT. Thus, the very broad change in G' (1 order of magnitude over 15 K change in temperature), should be due to the proximity of the SI-120 copolymer T_g to its ODT. Actually, the molecular characteristics of SI-120 are very similar to sample 2 in refs 19 and 53 (SI, $M_n = 10\,500$, $M_w/M_n = 1.04$, $f_{PS} = 0.50$), where only an estimate of the ODT could be obtained at ~330 K with the same if not bigger ambiguity than here. This value is in good agreement with the value (334 K) obtained from a correlation between ODT and N obtained for a series of symmetric

SI diblock copolymers.[39] Moreover, depolarized dynamic light scattering and static birefringence measurements do not show a clear discontinuous increase in the measured depolarized intensity or in the static birefringence but only a smooth change in the slope by crossing this temperature range, in disagreement with previous studies on both diblock copolymer solutions[31,55] and melts[30,56,57] far from their T_g's. More details on the static and dynamic light scattering investigations will be published elsewhere.[58] The estimated range for the ODT for SI-120 is on the right and outside the temperature range of Figure 9; i.e., the two processes are present at temperatures in the disordered state above the ODT, in agreement with the data for solution.[51]

IV. Discussion

The origin and mechanism of relaxation of the slower process observed for ordered diblocks will be discussed first in relation to Monte Carlo computer simulations[37] using the cooperative motion algorithm.[7,8,59] The analysis of the calculated correlation functions for the block end-to-end vector orientation for two symmetric diblocks with $N = 40$ and $N = 20$ ($f = 0.5$) and for an asymmetric with $N = 40$, $f = 0.25$ shows the presence of a single process (faster process) in the range of normal-mode processes for temperatures much higher than the estimated ODT, an extra shoulder in the distribution of relaxation times in the pretransitional regime near the ODT, and an extra slow process with a strong temperature dependence for temperatures below the ODT. Note that in the simulations the mobility of both species is independent of temperature, and thus, the temperature dependence is solely due to thermodynamics and not related to the proximity of the glass transition of the hard microphase.[21] Various findings of the simulation results lead to the assignment of the fast process to the normal-mode process of the subchain: (i) the associated relaxation times show an almost N^2 dependence between the two symmetric diblocks when compared at the same T/N, i.e., at the same distance from the Leibler's estimate of the ODT, and between those and the two different blocks for the asymmetric diblock; (ii) an almost N^2 dependence is also obeyed when the comparison is made between this process for the block orientation to the similar fast process for the chain end-to-end vector orientation both for the symmetric and the asymmetric system.

The slow process is observed for both the chain and the block orientation for both symmetric and asymmetric systems; however, (i) the relaxation times for this process are almost the same for the chain and the block orientation for the two symmetric systems, (ii) they are the same for the two different blocks and for the chain orientation for the asymmetric diblock, and (iii) a weak molecular weight dependence is observed between the $N = 20$ and $N = 40$ cases. The above computer simulation findings and the experimental fact that the intensity of this relaxation process but not its relaxation time depends on the coherence of the grains lead us to believe that the slow mode is due to a conformal motion of the interface plane perpendicular to the interface, which involves motions of the dielectrically active polyisoprene blocks, and thus, it can be observed by dielectric relaxation spectroscopy. This requires motion of whole chains in order to keep conformality, and thus, the time depends on the period of the microdomains which lead to an apparent molecular weight dependence. Indeed, the data in Figure 5 for the slow process show a slower relaxation rate for the diblock with the longer periodicity. These vibrational motions of the

interface plane affect both the block and the chain end-to-end vector correlation, and therefore, the simulations show the same correlation times for both. Apparently, although the intensity depends on the grain size, i.e., on how many chains move together, the respective relaxation times depend only on how much they have to move. The strong temperature dependence of the relaxation time of the process, which in the simulations is only due to thermodynamics, should be related to the increased unfavorable thermodynamic interactions as the temperature decreases, which leads to a slowing down of the process similar to the slowing down of the interdiffusion in polymer blends near the macrophase separation.[60] This strong temperature dependence should not be confused with the strong temperature dependence of the polystyrene segmental relaxation, which was experimentally found to be even stronger and definitely different from the slow process discussed here (Figure 5).

Below, an attempt is made to suggest a mechanism of relaxation that will explain the two processes observed for the SI-120 diblock in the disordered state near the ODT and the solutions in ref 51. The characteristic pertinent features of these processes are very strong, namely, the very weak temperature dependence of the relaxation rate of the faster process (Figure 9a), indicating a competition between mobility and thermodynamics, and the increase of the total dielectric strength by decreasing temperature (Figure 9b), which probably results from the extra correlations in the proximity of the ODT due to orientation and/or extension of the polymer chains near the ODT.

A theoretical approach was presented in ref 20 in order to calculate the distribution of relaxation times for the block end-to-end vector orientation correlations by considering both the short-range fluctuations due to chain connectivity and the long-range concentration fluctuations in diblock copolymers due to the proximity to the ODT and their coupling to the individual block segmental dynamics. Theory was in quantitative agreement with the experimental dielectric loss spectra for a series of well-disordered diblock copolymer melts.[20] In that work, the probability density for the composition fluctuations averaged over an n-segment subchain of the copolymer block was assumed to be Gaussian, with a variance $\sigma_n^2 = \int S(\mathbf{q}) g_n(-\mathbf{q}) \, d\mathbf{q}/(2\pi)^3$ related to the thermodynamics via the structure factor $S(q)$, where $g_n(q)$ is the Debye function for an n-segment subchain. The assumption of the Gaussian form of the distribution leads to the prediction of a unimodal distribution of relaxation times with a width that is affected by both the thermodynamics and the proximity to the glass transitions of the individual components. Actually, for a symmetric diblock near the ODT, the above approach predicts[20] a width of the relaxation spectrum, $\Delta(\ln \tau) \propto CN^{-1/4}\epsilon_t^{-1/4}$, where $\epsilon_t = (\chi_s - \chi)N$ denotes the proximity to the ODT with χ_s the value of the interaction parameter at Leibler's stability limit and C a factor that relates local volume fraction to local mobility.[20] Prediction of a bimodal distribution of relaxation times could only be obtained if the probability density for the composition fluctuations assumes a bimodal form.

A possible mechanism for the observed behavior may be related to the extra orientational correlations of chains in the proximity to the ODT. As the ODT is approached, the composition fluctuations lead to equilibrium field configurations ("pattern") that fluctuate in time and that were speculated[4] to be reminiscent of the transient nonequilibrium patterns encountered during the intermediate and late stages of spinodal decomposi-

tion,[61] based on a reconstruction of the structure factor.[62] Polyisoprene chains may, therefore, be considered as essentially anchored to the pseudointerfaces with the much slower polystyrene-rich environments. For a complete polyisoprene block orientational relaxation and besides the faster relaxation due to motions of the free ends in the isoprene-rich microdomains, the pseudointerface planes should also relax. The correlation times of such motion should be similar to the relaxation of composition fluctuations with wave vectors in the proximity of the maximum of the structure factor, q^*. This mechanism of relaxation of the polyisoprene blocks is similar to the mechanism that leads to a slow process[30] in depolarized dynamic light scattering due to the orientation and/or extension of the copolymer chains in the pretransitional regime above the ODT with the relevant length scale of the slow orientation fluctuations being close to $2\pi/q^*$. Indeed, the computer simulations[37] showed that the correlation times of the slow relaxation in the block end-to-end vector correlation functions are close to those in the concentration correlation function. Experimentally, the correlation times of the slow process in depolarized light scattering[30] were by about 3–4 orders of magnitude slower than the segmental times of the polystyrene-rich microenvironment. Note that depolarized light scattering is sensitive to polystyrene reorientation due to the much higher optical anisotropy of the styrene than the isoprene segments; therefore, the rate of the process observed by light scattering was controlled by the segmental times of the polystyrene environment. In contrast, dielectric relaxation is monitoring the relaxations through the dipole moment of the isoprene segments, and for well disordered diblocks, the relaxation rate of the polyisoprene block end-to-end vector relaxation was determined[35] by the average friction of the melt, which for SI-100 should be by about $N_{I,SI\text{-}100}^2$ or 3.2 orders faster than the normal mode in Figure 9. The motion of the interface planes, discussed herein, should also be determined by the average friction due to the mixing at the interphase. This means that the relaxation rate of the slower process for SI-120 in Figure 8 should be by about 3–4 orders slower than the average segmental times. Therefore, the relaxation times of the slow dielectric process should indeed be similar to those for the normal mode of SI-100 as in Figure 9.

This mechanism suggests that the slower process in SI-120 is due to the induced orientational correlations in the proximity of the ODT and that the faster process is related to the usual normal-mode process due to motion of the polyisoprene free ends in the isoprene-rich microdomain. The weak temperature dependence of this process implies the existence of two competing factors, i.e., a kinetic slowing-down due to reduced mobility by decreasing temperature toward the glass transition and a thermodynamic speed-up due to the isoprene-rich regions becoming richer in isoprene due to thermodynamics, as the composition fluctuations increase in amplitude when the ODT is approached.

At this stage, we would attempt to summarize the behavior of the block end-to-end vector relaxation in diblock copolymers as one moves from the well disordered all the way to the ordered state. Unfortunately, due to the limited time windows of the experimental techniques, one is not able to experimentally observe this behavior over the whole temperature range required. However, an attempt can be made to address this issue by utilizing measurements for a series of diblock copolymers of different molecular weights. In order to reduce the temperature axis, we have chosen

the variable $\epsilon(N,T) = [N/T - N/T_{ODT}]$, which is proportional to the $N(\chi - \chi_s)$ parameter that in the mean field describes the thermodynamic state of diblock copolymers.[2] In this approximation, one neglects any molecular weight and concentration effects on χ; we will utilize more-or-less symmetric diblocks and thus the assumption of neglecting the composition dependence of χ is not so severe. Moreover, we have neglected in this comparison the effects of the Brazovskii fluctuation corrections that introduce[3] a correction of $O(\bar{N}^{-1/3})$ to the χN parameter in order to describe the thermodynamic state.

There are two reductions that have to be taken into account with respect to the relaxation rate axis; one is the dependence of the times on the molecular weight (for normal mode in the Rouse regime a N_{PI}^2 factor) and the differences in the local frictions that determine the dynamics in the different thermodynamic regimes. For the former we neglect the corrections for two reasons: first, the molecular weights of the polyisoprene blocks are very low and not so different, and second the molecular weight dependence of the extra processes observed for SI-120, SI-194, and SI-144 are not known. With respect to the local friction normalization, one should scale the normal-mode times to an isofrictional state. For specimens well in the disordered state, it has been found that it is the average segmental time that when scaled with the block molecular weight determines[35] the polyisoprene block end-to-end vector relaxation measured by dielectric relaxation spectroscopy. In the ordered state, on the other hand, the polyisoprene block relaxation times are only slightly slower[21] (a little over a factor of 4) than the normal mode of polyisoprene homopolymer chains of equivalent molecular weights, as is also shown in Figure 5; i.e., the dynamics is determined by pure polyisoprene segmental times. For the SI-120 specimen in the strong fluctuations regime, the polyisoprene blocks should be feeling a local friction that changes with temperature between the average environment at higher temperatures to that of more-isoprene rich as the ODT is approached. Comparing data for the two ordered diblock copolymers at the same thermodynamic state, i.e., at the same $[N/T - N/T_{ODT}]$, results in comparing data at essentially different absolute temperatures and, therefore, at a different distance from the respective glass transition temperatures. Therefore, when plotting the data for SI-144 in the same graph with SI-194, one should correct by scaling the frictions for SI-144 to those at the equivalent temperature, T', for SI-194 given by $\epsilon(144,T) = \epsilon(194,T')$. Finally, the data for SI-100 should be scaled to the friction of pure isoprene, which determines the relaxation for SI-194, as $\tau_r = \tau_n(\tau_{0,PI}/\tau_{0,av})$, with the average local time calculated as discussed before.[35]

In Figure 10 we present the composite relaxation map for the disordered SI-100, the ordered SI-194 and SI-144, and the specimen SI-120 in the intermediate regime vs $\epsilon(N,T) = [N/T - N/T_{ODT}]$; the ODT corresponds to $\epsilon(N,T) = 0$. The observed behavior resembles that estimated on the basis of the computer simulation results as discussed in another publication.[37] The single block end-to-end vector orientation process well in the disordered state splits into two processes as the ODT is approached: a faster process due to motion of the free ends and a slower process due to extra orientational correlations. Below the ODT, the fast process is the usual block end-to-end vector orientation within the ordered microdomains whereas the slow process, which is not necessary a continuation of the slower process above the ODT, is related to the relaxation of the
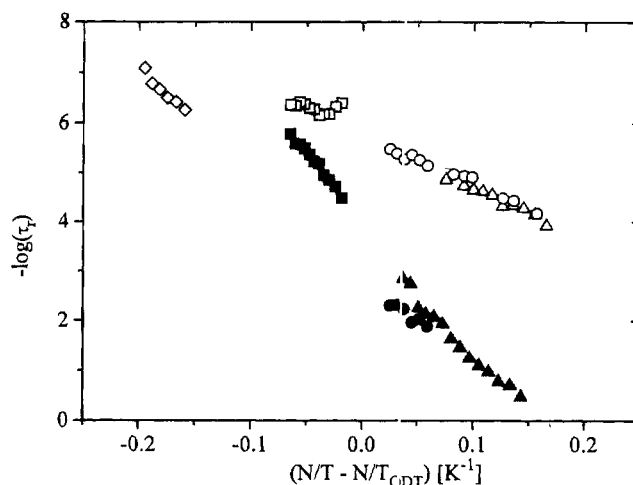

Figure 10. Composite relaxation map for diblock copolymers SI-100 ($\Diamond$), SI-120 ($\Box$, $\blacksquare$), SI-144 (O, $\bullet$), and SI-194 ($\triangle$, $\blacktriangle$) as a function of the thermodynamic state of the system ($\epsilon(N,T)$ $= [N/T - N/T_{ODT}]$ is taken to be equivalent to $[\chi N - (\chi N)_s]$ in this respect). The relaxation times for SI-100 are scaled with the ratio of the effective average segmental times to the segmental times of the polyisoprene-rich environment (see text) whereas the data for SI-144 are scaled to the isofriction state with SI-194 (see text).

interfacial planes formed in the ordered state.

V. Concluding Remarks

The block end-to-end vector orientation correlations in symmetric diblock copolymers both in the ordered state and in the disordered state close to the order-to-disorder transition have been investigated by dielectric relaxation spectroscopy. The behavior for well-disordered diblock copolymers was addressed in an earlier publication.[20] In the ordered state, a new block relaxation appears with amplitude depending on the sample preparation, slow dynamics, and strong temperature dependence. Utilizing a comparison with Monte Carlo computer simulations, the slow process is attributed to the relaxation of the conformal interfaces formed in the ordered state within the grains of coherently ordered lamellae. When the ODT is approached from the disordered state by decreasing temperature, a bifurcation of the single dielectric normal-mode relaxation is observed. The low-frequency relaxation displays temperature dependence similar to the temperature dependence of dielectric normal-mode relaxation far from the ODT, whereas the high-frequency component shows an apparent weak temperature dependence. The total dielectric strength of the two processes increases as the temperature decreases. The fast process may be related to polyisoprene chains that feel higher polyisoprene concentrations near the ODT due to the increased amplitude of composition fluctuations, whereas the slow process should be attributed to the extra orientation correlations near the ODT as supported also by computer simulations. Finally, a composite diagram is proposed to summarize the dielectric relaxation behavior of the block end-to-end vector orientation correlation as a function of the thermodynamic state of a diblock copolymer from well in the disordered to well in the ordered state.

References and Notes

(1) Bates, F. S.; Fredrickson, G. H. *Annu. Rev. Phys. Chem.* **1990**, *41*, 525.

(2) Leibler, L. *Macromolecules* **1980**, *13*, 1602.

(3) (a) Fredrickson, G. H.; Helfand, E. *J. Chem. Phys.* **1987**, *87*, 697. (b) Barrat, G. L.; Fredrickson, G. H. *J. Chem. Phys.* **1991**, *95*, 1282.

(4) Bates, F. S.; Rosedale, J. H.; Fredrickson, G. H. *J. Chem. Phys.* **1990**, *92*, 6255. Rosedale, J. H.; Bates, F. S. *Macromolecules* **1990**, *23*, 2329. Rosedale, J. H.; Bates, F. S.; Almdal, K.; Mortensen, K.; Wignall, G. D. *Macromolecules* **1995**, *28*, 1429.

(5) Fried, H.; Binder, K. *Europhys. Lett.* **1991**, *16*, 237; *J. Chem. Phys.* **1991**, *94*, 8349.

(6) Binder, K.; Fried, H. *Macromolecules* **1993**, *26*, 6878.

(7) Gauger, A.; Weyersberg, A.; Pakula, T. *Makromol. Chem., Theory Simul.* **1993**, *2*, 531.

(8) Weyersberg, A.; Vilgis, T. A. *Phys. Rev. E* **1993**, *48*, 377.

(9) Pakula, T. *Makromol. Chem., Theory Simul.* **1993**, *2*, 239.

(10) Larson, R. G. *Macromolecules* **1994**, *27*, 4198.

(11) Fytas, G.; Anastasiadis, S. H. In *Disorder Effects on Relaxation Processes*; Richert, R., Blumen, A., Eds.; Springer Verlag: Berlin, 1993.

(12) Akcasu, A. Z.; Benmouna, M.; Benoit, H. *Polymer* **1986**, *27*, 1935. Akcasu, A. Z.; Tombakoglu, M. *Macromolecules* **1990**, *23*, 607. Akcasu, A. Z. *Macromolecules* **1991**, *24*, 2109. Borsali, R.; Vilgis, T. A. *J. Chem. Phys.* **1990**, *93*, 3610.

(13) Fredrickson, G. H.; Helfand, E. *J. Chem. Phys.* **1988**, *89*, 5890. Fredrickson, G. H. *J. Chem. Phys.* **1986**, *85*, 5306. Fredrickson, G. H.; Larson, R. G. *Macromolecules* **1987**, *20*, 1897. Onuki, A. *J. Chem. Phys.* **1987**, *87*, 3692.

(14) Quan, X.; Johnson, G. E.; Anderson, E. W.; Bates, F. S. *Macromolecules* **1989**, *22*, 2451.

(15) Kanetakis, J.; Fytas, G.; Kremer, F.; Pakula, T. *Macromolecules* **1992**, *25*, 3484. Rizos, A.; Fytas, G.; Roovers, J. C. *J. Chem. Phys.* **1992**, *97*, 6925.

(16) Anastasiadis, S. H.; Fytas, G.; Vogt, S.; Gerharz, B.; Fischer, E. W. *Europhys. Lett.* **1993**, *26*, 619.

(17) Vogt, S.; Gerharz, B.; Fischer, E. W.; Fytas, G. *Macromolecules* **1992**, *25*, 5986.

(18) Alig, I.; Kremer, F.; Fytas, G.; Roovers, J. C. *Macromolecules* **1992**, *25*, 5277.

(19) Stühn, B.; Stickel, F. *Macromolecules* **1992**, *25*, 5306.

(20) Karatasos, K.; Anastasiadis, S. H.; Semenov, A. N.; Fytas, G.; Pitsikalis, M.; Hadjichristidis, N. *Macromolecules* **1994**, *27*, 3543.

(21) Yao, M.-L.; Watanabe, H.; Adachi, K.; Kotaka, T. *Macromolecules* **1991**, *24*, 2955.

(22) Yao, M.-L.; Watanabe, H.; Adachi, K.; Kotaka, T. *Macromolecules* **1992**, *25*, 1699.

(23) Borsali, R.; Benoit, H.; Legrand, J.-F.; Duval, M.; Picot, C.; Benmouna, M.; Farago, B. *Macromolecules* **1989**, *22*, 4119. Duval, M.; Picot, C.; Benoit, H.; Borsali, R.; Benmouna, M.; Lartigue, C. *Macromolecules* **1991**, *24*, 3185.

(24) Anastasiadis, S. H.; Fytas, G.; Vogt, S.; Fischer, E. W. *Phys. Rev. Lett.* **1993**, *70*, 2415.

(25) Vogt, S.; Anastasiadis, S. H.; Fytas, G.; Fischer, E. W. *Macromolecules* **1994**, *27*, 4335.

(26) Jian, T.; Anastasiadis, S. H.; Semenov, A. N.; Fytas, G.; Adachi, K.; Kotaka, T. *Macromolecules* **1994**, *27*, 4762. Fytas, G.; Anastasiadis, S. H.; Semenov, A. N. *Makromol. Chem., Macromol. Symp.* **1994**, *79*, 117.

(27) Vogt, S.; Jian, T.; Anastasiadis, S. H.; Fytas, G.; Fischer, E. W. *Macromolecules* **1993**, *26*, 3357.

(28) Jian, T.; Anastasiadis, S. H.; Fytas, G.; Fleischer, G.; Vilesov, A. D. *Macromolecules* **1995**, *28*, 2439.

(29) Balsara, N. P.; Stepanek, P.; Lodge, T. P.; Tirrell, M. *Macromolecules* **1991**, *24*, 6227. Balsara, N. P.; Eastman, C.

(30) E.; Foster, M. D.; Lodge, T. P.; Tirrell, M. *Makromol. Chem., Macromol. Symp.* **1991**, *45*, 213. Pan, C.; Maurer, W.; Liu, Z.; Lodge, T. P.; Stepanek, P.; von Meerwall, E. D.; Watanabe, H. *Macromolecules* **1995**, *28*, 1643.

(30) Jian, T.; Semenov, A. N.; Anastasiadis, S. H.; Fytas, G.; Feh, F.-J.; Chu, B.; Vogt, S.; Wang, F.; Roovers, J. E. L. *J. Chem. Phys.* **1994**, *100*, 3286.

(31) Jian, T.; Anastasiadis, S. H.; Fytas, G.; Adachi, K.; Kotaka, T. *Macromolecules* **1993**, *26*, 4706.

(32) Ehlich, D.; Takenaka, M.; Okamoto, S.; Hashimoto, T. *Macromolecules* **1993**, *26*, 189. Ehlich, D.; Takenaka, M.; Hashimoto, T. *Macromolecules* **1993**, *26*, 492. Dalvi, M. C.; Lodge, T. P. *Macromolecules* **1993**, *26*, 859; **1994**, *27*, 3487.

(33) Shull, K. R.; Kramer, E. J.; Bates, F. S.; Rosedale, J. H. *Macromolecules* **1991**, *24*, 1383.

(34) Fleischer, G.; Fujara, F.; Stühn, B. *Macromolecules* **1993**, *26*, 492.

(35) Fytas, G.; Anastasiadis, S. H.; Karatasos, K.; Hadjichristidis, N. *Phys. Scr.* **1993**, *T49*, 237.

(36) Stockmayer, W. H. *Pure Appl. Chem.* **1967**, *15*, 539.

(37) Pakula, T.; Karatasos, K.; Anastasiadis, S. H.; Fytas, G. *Macromolecules*, submitted for publication.

(38) Floudas, G.; Pakula, T; Fischer, E. W.; Hadjichristidis, N.; Pispas, S. *Acta Polym.* **1994**, *45*, 176.

(39) Floudas, G.; Vlassopoulos, D.; Pitsikalis, M.; Hadjichristidis, N.; Stamm, M. *J. Chem. Phys.*, in press.

(40) Cole, R. H. *J. Chem. Phys.* **1965**, *42*, 637.

(41) Bauer, M. E.; Stockmayer, W. H. *J. Chem. Phys.* **1965**, *43*, 4319. Adachi, K.; Kotaka, T. *Macromolecules* **1985**, *18*, 466. Boese, D.; Kremer, F. *Macromolecules* **1990**, *23*, 829.

(42) Adachi, K.; Kotaka, T. *Macromolecules* **1988**, *21*, 157. Adachi, K.; Kotaka, T. *Prog. Polym. Sci.* **1993**, *18*, 585.

(43) Boese, D.; Kremer, F. *Macromolecules* **1990**, *23*, 829.

(44) Havriliak, S.; Negami, S. *Polymer* **1967**, *8*, 161.

(45) Imanishi, Y.; Adachi, K.; Kotaka, T. *J. Chem. Phys.* **1988**, *89*, 7593. Liedermann, K.; Loidl, A. *J. Non-Cryst. Solids* **1993**, *155*, 26. Alvarez, F.; Alegria, A.; Colmenero, J. *J. Chem. Phys.* **1995**, *103*, 798. Schäfer, H.; Sternin, E.; Stannarius, R.; Arndt, M.; Kremer, F. *Phys. Rev. B*, submitted for publication.

(46) Provencher, S. W. *Comput. Phys. Commun.* **1982**, *27*, 213; **1982**, *27*, 229.

(47) Fytas, G.; Meier, G. In *Dynamic Light Scattering*; Brown, W., Ed.; Oxford University Press: Oxford, U.K., 1993; Chapter 9, p 407.

(48) Alvarez, F.; Alegria, A.; Colmenero, J. *J. Chem. Phys.* **1995**, *103*, 798.

(49) Floudas, G.; Pakula, T; Stamm, M.; Fischer, E. W. *Macromolecules* **1993**, *26*, 1671.

(50) Floudas, G.; Vogt, S.; Pakula, T; Fischer, E. W. *Macromolecules* **1993**, *26*, 7210.

(51) Adachi, K., unpublished data.

(52) Hashimoto, T.; Todo, A.; Itoi, H.; Kawai, H. *Macromolecules* **1977**, *10*, 377. Hashimoto, T.; Shibayama, M.; Kawai, H. *Macromolecules* **1980**, *13*, 1237. Hashimoto, T.; Tanaka, H.; Itoi, H.; Hasegawa, H. *Macromolecules* **1985**, *18*, 1864.

(53) Stühn, B. *J. Polym. Sci.: Part B: Polym. Phys.* **1992**, *30*, 1013.

(54) Meier, G.; Vlassopoulos, D.; Fytas, G. *Europhys. Lett.* **1995**, *30*, 325.

(55) Balsara, N. P.; Perahia, D.; Safinya, C. R.; Tirrell, M.; Lodge, T. P. *Macromolecules* **1992**, *25*, 3896.

(56) Amundson, K.; Helfand, E.; Patel, S. S.; Quan, X.; Smith, S. D. *Macromolecules* **1992**, *25*, 1935.

(57) Floudas, G.; Fytas, G.; Hadjichristidis, N.; Pitsikalis, M. *Macromolecules* **1995**, *28*, 2359.

(58) Karatasos, K.; Jian, T.; Fytas, G.; Anastasiadis, S. H.; Hadjichristidis, N.; Roovers, J. E. L., in preparation.

(59) Pakula, T. *Macromolecules* **1987**, *20*, 679. Pakula, T.; Geyler, S. *Macromolecules* **1987**, *20*, 2909.

(60) Meier, G.; Fytas, G.; Momper, B.; Fleischer, G. *Macromolecules* **1993**, *26*, 5310, and references therein. Jordan, E. A.; Ball, R. C.; Donald, A. M.; Fetters, L. J.; Jones, R. A. L.; Klein, J. *Macromolecules* **1988**, *21*, 235. Composto, R. J.; Kramer, E. J.; White, D. M. *Macromolecules* **1988**, *21*, 2580. Kanetakis, J.; Fytas, G. *Macromolecules* **1989**, *22*, 3452.

(61) Bates, F. S.; Wiltzius, P. *J. Chem. Phys.* **1989**, *91*, 3258.

(62) Berg, N. F. *Phys. Rev. Lett.* **1987**, *58*, 2718.